

Caffeine-Mediated Detachment of Mutagenic Ethidium from Various Nanoscopic Micelles: An Ultrafast Förster Resonance Energy Transfer Study

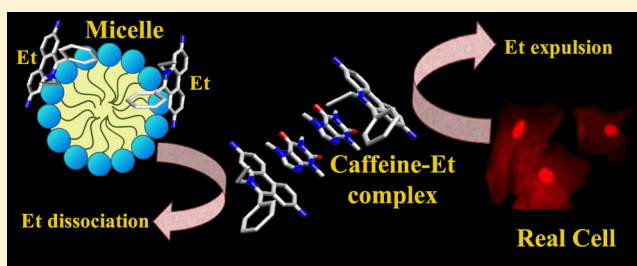
Soma Banerjee,[†] Masanori Tachiya,[‡] and Samir Kumar Pal^{*,†}

[†]Department of Chemical, Biological & Macromolecular Sciences, S. N. Bose National Centre for Basic Sciences, Block JD, Sector III, Salt Lake, Kolkata 700 098, India

[‡]National Institute of Advanced Industrial Science and Technology (AIST), Tsukuba Ibaraki 305-8565, Japan

S Supporting Information

ABSTRACT: In the present study we explore the efficacy of caffeine in dissociating the ethidium (Et) molecule, a model DNA-intercalator as well as a potential mutagen, from nanometer sized micelles of various charges. Steady-state and picosecond-resolved spectroscopic studies on the detachment of Et from various biomimicking micelles of different charges (cationic hexadecyltrimethylammonium bromide (CTAB), neutral (polar) Triton X-100 (TX-100), and anionic sodium dodecyl sulfate (SDS)) reveal the specificity of the caffeine molecule for carrying out such dissociation. The picosecond-resolved Förster resonance energy transfer (FRET) studies between a DNA minor groove binder dye Hoeschst 33258 (H2S8, donor) and Et (acceptor) have been employed to investigate the alteration in their association in the presence of caffeine at the molecular level. Analysis of our experimental results employing both the generalized and the extended version of the well-known “Infelta–Tachiya model” vividly illustrates how the distribution of Et along with the equilibrium constant of its solubilization in the micelle changes in the presence of caffeine in aqueous solution. Finally, our fluorescence micrographs of squamous epithelial cells validate the alteration of FRET efficiency between the donor and the acceptor due to the release of the latter in the presence of caffeine.



INTRODUCTION

The molecular recognition of DNA by small ligands/drugs in the presence of caffeine, a xanthine alkaloid, in aqueous solution is well-known.^{1–3} Earlier it is shown that the intercalation of novantrone, ellipticine, doxorubicin, and ethidium bromide to DNA is significantly perturbed in the presence of caffeine.^{2,4,5} Other studies also reveal similar observations.^{6–8} A detailed spectroscopic investigation from our laboratory⁹ demonstrates the efficacy of caffeine in the removal of Et from synthetic self-complementary oligonucleotides and from different cell lines. The significant alteration of molecular recognition of DNA in caffeine solution has been concluded to depend on the “protector” and “interceptor” properties of caffeine.^{4,5,10} In the “protector” mode of activity, there is a strong competition between caffeine and aromatic drug for the binding sites on DNA whereas in the “interceptor” mode of its activity, caffeine forms heterocomplexes with a number of aromatic DNA intercalators, which account for the observed changes of biological activity of these drugs in the presence of caffeine. Sometimes, explanation of specific role of caffeine in the molecular recognition of DNA in physiological milieu becomes cumbersome.¹⁰ In this regard small biomimetic systems including nanoscopic micelles¹¹ could serve as an efficient mimic for the biological membranes and macromolecules and

are also useful in organizing the reactants at a molecular level.¹¹ For example, the cationic hexadecyltrimethylammonium bromide (CTAB) micelle may act as a good mimic of histone protein,¹² the neutral (polar) Triton X-100 (TX-100) micelle may mimic a protein cavity,¹³ and the anionic sodium dodecyl sulfate (SDS) micelle can serve as a good alternative of the DNA surface.^{14,15} To date, however, no attempt has been made to use nanoscopic micelles for the better understanding of caffeine-mediated molecular recognition of DNA by small ligands/drugs and is the motive of our present study.

In the present study we have used ethidium (Et) bromide salt as model ligand probe, which is a well-known DNA intercalator^{16,17} and a potential mutagen.¹⁸ The micelles used in our study are cationic CTAB, neutral (polar) TX-100, and anionic SDS with distinct hydrodynamic diameter as measured by dynamic light scattering (DLS) experiment. The probe Et shows a distinct spectroscopic signature, particularly the excited-state lifetime in various biologically relevant environments. We have used steady-state and picosecond-resolved fluorescence spectroscopy to investigate the detachment of Et from various self-organized micelles. In the case of DNA

Received: December 5, 2011

Published: June 11, 2012

mimicking SDS micelles we have used another probe Hoechst 33258 (H258) as energy donor to Et acceptor at the surface and employ FRET (Förster resonance energy transfer) for the analysis of fluorescence quenching of the donor H258. Standard FRET analysis on the donor–acceptor (D–A) pair at the SDS micelle shows significant perturbation on the energy transfer efficiency upon addition of caffeine in the solution. Further analysis of the experimental results employing both the general and extended version of well-known “Infelta–Tachiya model” distinctly reveals a change in acceptor distribution at the micellar surface in the presence of caffeine in the aqueous solution. We have used DLS to confirm the structural integrity of the micelles in the caffeine solution. Furthermore, we have employed fluorescence microscopy to monitor the said perturbation in FRET efficiency on squamous epithelial cell nuclei in the presence of caffeine.

MATERIALS AND METHODS

The fluorescent dyes Hoechst 33258 (H258) and ethidium (Et) bromide were obtained from Molecular Probes whereas caffeine and hexadecyltrimethylammonium bromide (CTAB) were from Fluka. Sodium dodecyl sulfate (SDS) and Triton X-100 (TX-100) were acquired from Fisher Scientific and Romil, respectively; coumarin 500 (C500) was from Exciton and used without further purification. The concentration of caffeine used in our present study, excluding the cellular work, is 100 mM because it is the maximum concentration achievable at room temperature in aqueous phase and optimum detachment of Et from the micellar surfaces can be demonstrated. For cellular study the concentration of caffeine used is 10 mM. All the solutions were prepared in double distilled water, except for cellular studies where the samples were prepared in phosphate buffer saline (PBS, pH 7.4) using double distilled water. Squamous epithelial cells were collected from human mouth and spread on glass slides and doubly stained with H258 and Et followed by thorough destaining with PBS each time after staining.

Fluorescence micrographs were taken using an Olympus BX51 fluorescence microscope connected with DP72 microscope digital camera. The Olympus fluorescence microscope is equipped with various sets of fluorescence mirror unit combined with appropriate filters that are variable depending on wavelengths. The fluorescence mirror unit that matches the fluorochrome in use was selected. Cells were irradiated under UV light at 360 nm continuously for 800 s. All the images were taken under 50× magnification. The micrographs were analyzed with analySIS Five image analysis software provided with the microscope. The software was used to measure the intensity of red, green, and blue component in each micrograph. Steady-state absorption and emission were measured with Shimadzu Model UV-2450 spectrophotometer and Jobin Yvon Model Fluoromax-3 fluorometer, respectively. All picosecond transients were measured by using commercially available (Edinburgh Instrument, UK) picosecond-resolved time correlated single photon counting (TCSPC) setup (instrument response function (IRF) of 80 ps) using 375 nm (λ_{ex}) excitation laser source and all the fluorescence transients of the donor H258 and the donor C500 have been monitored at 470 nm (λ_{em}) and 500 nm (λ_{em}), respectively. It has to be noted that, with our time-resolved instrument, we can resolve at least one-fourth of the instrument response time constants after the deconvolution of the IRF. Fluorescence from the sample was detected by a photomultiplier after dispersing through a double

grating monochromator. For all transients the polarizer in the emission side was adjusted to be at 54.7° (magic angle) with respect to the polarization axis of the excitation beam. To estimate the Förster resonance energy transfer (FRET) efficiency of the donor (H258) to the acceptor (Et) and, hence, to determine distances of donor–acceptor (D–A) pairs, we have followed the methodology described in chapter 13 of ref 19. The Förster distance (R_0) is given by

$$R_0 = 0.211[\kappa^2 n^{-4} Q_D J(\lambda)]^{1/6} \text{ (in Å)} \quad (1)$$

where (κ^2) is a factor describing the relative orientation in space of the transition dipoles of the donor and acceptor. The value of the orientation factor (κ^2) is calculated from the equation

$$\kappa^2 = (\cos \theta_T - 3 \cos \theta_D - \cos \theta_A) \quad (2)$$

where θ_T is the angle between the emission transition dipole of the donor and absorption transition dipole of the acceptor and θ_D and θ_A are the angles between these dipoles and the vector joining the donor and acceptor.¹⁹ In the micellar system, the donor and acceptor molecules can be bound simultaneously without any restriction on the relative orientation of their transition dipole moments. According to our proposed model (see below), the positively charged part of the dye Et is located toward the negatively charged headgroup of the SDS micelle and the hydrophobic part of the dye is buried inside. Because one part of the dye is attached to the negatively charged surface of the micelle and the other part of the dye is free, the dye can adopt all possible orientations. Thus, the orientation parameter (κ^2) can be taken as 0.667.¹⁹ Moreover, because the sixth root is taken to calculate the distance, variation, of κ^2 from the value for random orientation ($\kappa^2 = 2/3$) to that for parallel dipolar orientation ($\kappa^2 = 1$) or to that for head-to-tail parallel transition dipoles ($\kappa^2 = 4$), the calculated distance can be in error by no more than 35%.¹⁹ The refractive index (n) of the medium is assumed to be 1.4. Q_D , the quantum yield of the donor H258 in the absence of acceptor Et in the SDS micelle, is 0.54 and 0.3 in the absence¹⁷ and presence of caffeine, respectively. $J(\lambda)$, the overlap integral, which expresses the degree of spectral overlap between the donor H258 emission and the acceptor Et absorption, is given by

$$J(\lambda) = \frac{\int_0^\infty F_D(\lambda) \epsilon(\lambda) \lambda^4 d(\lambda)}{\int_0^\infty F_D(\lambda) d(\lambda)} \quad (3)$$

where $F_D(\lambda)$ is the fluorescence intensity of the donor in the wavelength range of λ to $\lambda + d\lambda$ and is dimensionless. $\epsilon(\lambda)$ is the extinction coefficient (in $\text{M}^{-1} \text{cm}^{-1}$) of the acceptor at λ . If λ is in nm, then $J(\lambda)$ is in units of $\text{cm}^{-1} \text{nm}^4$. Once the value of R_0 is known, the D–A distance (r) can easily be calculated using the formula,

$$r^6 = [R_0^6(1 - E)]/E \quad (4)$$

Here, E is the efficiency of energy transfer. The efficiency (E) is calculated from the lifetimes of the donor in the absence and presence of acceptors (τ_D and τ_{DA}).

$$E = 1 - \frac{\tau_{DA}}{\tau_D} \quad (5)$$

The longer lifetime component in the decay of the D–A pair that resembles the decay component of the donor alone is due to less than 100% labeling by acceptor¹⁹ and has not been considered while τ_{DA} is calculated. To prevent homomolecular

energy transfer between donor molecules and to ensure efficient energy transfer between the donor and acceptor, the concentration of the donor molecules is kept low ($0.2 \mu\text{M}$) whereas that of the acceptor molecules is $155 \mu\text{M}$, which is comparable to the micellar concentration of $194 \mu\text{M}$ (surfactant SDS concentration being 20 mM).

Dynamic light scattering (DLS) measurements were done with Nano S Malvern instruments employing a 4 mW He–Ne laser ($\lambda = 632.8 \text{ nm}$) equipped with a thermostatted sample chamber. All measurements are taken at 173° scattering angle and at 25°C . The scattering intensity data are processed using the instrumental software to obtain the hydrodynamic diameter (d_{H}) and the size distribution of the scatterer in each sample. The instrument measures the time-dependent fluctuation in intensity of light scattered from the particles in solution at a fixed scattering angle. Hydrodynamic diameters (d_{H}) of the particles are estimated from the intensity auto correlation function of the time-dependent fluctuation in intensity. d_{H} is defined as

$$d_{\text{H}} = \frac{kT}{3\pi\eta D} \quad (6)$$

where k is the Boltzmann constant, T is the absolute temperature, η is viscosity, and D is the translational diffusion coefficient. In a typical size distribution graph from the DLS measurement, the X-axis shows a distribution of size classes in nanometers, whereas the Y-axis shows the relative intensity of the scattered light.

RESULTS AND DISCUSSION

Figure 1a shows the fluorescence transients of the mutagenic ethidium (Et) in various micellar systems of different charge nature in the absence and presence of caffeine. Both Et and CTAB being cationic, ionic interaction between the two will not be favored but the possibility of hydrophobic interaction between them cannot be ruled out. This was the reason behind our selection of cationic CTAB and neutral (polar) TX-100 micelles. As evidenced from our lifetime results (given in Supporting Information section, Table S1), beyond the critical micelle concentration (CMC) of CTAB, Et interacts with the micelle to some extent, which is only possible through its interior binding. Et in the cationic CTAB micelles reveals fluorescence lifetimes of 1.4 ns (51%) and 2.5 ns (49%). However, on addition of caffeine in the solution, the lifetime values become 1.9 ns (14%) and 7.2 ns (86%), revealing a major slower component (7.2 ns), characteristic of Et–caffeine complexation (Table 1). The faster component is close to the lifetime of Et in water, which is $\sim 1.5 \text{ ns}$.¹⁶ In the case of anionic SDS micelles significant detachment of Et in the caffeine solution is also evident (Figure 1a and Table 1). Our SDS concentration dependent absorption studies along with the time-resolved fluorescence and anisotropy measurements on Et both in the absence and in the presence of caffeine (details given in Supporting Information section, Figure S1 and Table S2) is in good agreement with the model where Et attaches to the SDS micelle with its positively charged moiety toward the negatively charged headgroup of the SDS micelle and hydrophobic part inside the micelle. From the difference in optical density (OD) value of Et in the SDS micelle in the absence and presence of caffeine, we calculated the amount of Et released from the micelle by caffeine taking the molar extinction coefficient of Et in the SDS micelle as 4120 M^{-1}

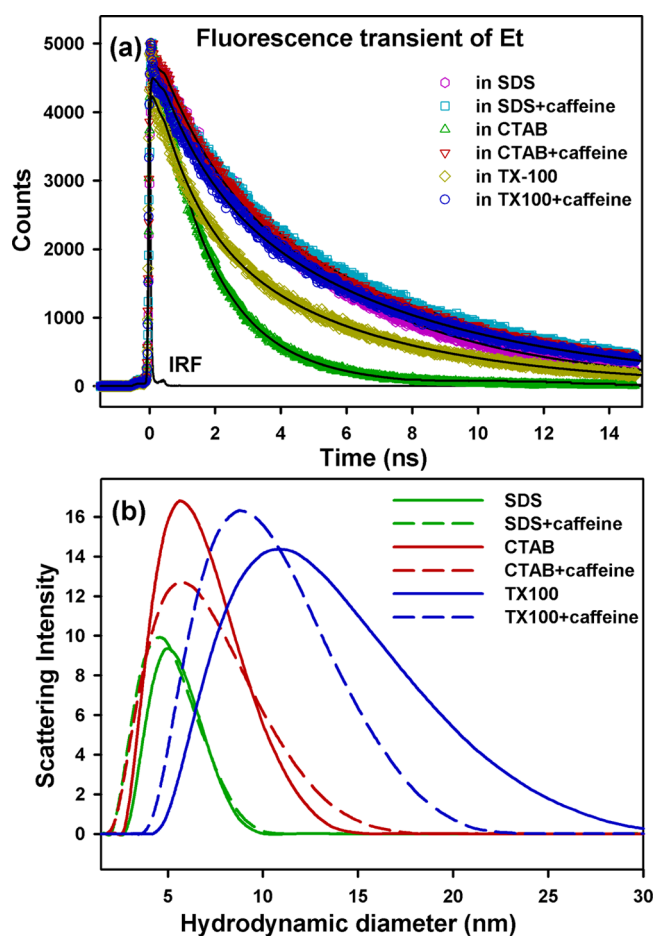


Figure 1. (a) Fluorescence transients of Et in SDS, CTAB, and TX-100 micellar systems and (b) diameter size of those micelles, in the presence and absence of caffeine.

Table 1. Lifetime Components of Ethidium (Et) in Aqueous Solvent and in Micellar Compartments with and without Caffeine^a

sample	τ_1 (ns)	τ_2 (ns)
Et in water	1.6 (100%)	
Et in aqueous caffeine solution	7.0 (84.5%)	2.3 (15.5%)
Et in CTAB	1.4 (51%)	2.46 (49%)
Et in CTAB + caffeine	1.9 (14%)	7.2 (86%)
Et in SDS	1.46 (5%)	5.15 (95%)
Et in SDS + caffeine	2.06 (12%)	7.25 (88%)
Et in TX-100	1.21 (16%)	5.37 (84%)
Et in TX-100 + caffeine	1.45 (10%)	6.77 (90%)

^a τ represents the time constant, and the numbers in parentheses represent relative contribution of the component. Surfactant as well as caffeine concentrations maintained at 100 mM . Error $\pm 5\%$.

cm^{-1} at 476 nm . It has been found that from $25 \mu\text{M}$ micelle-bound EtBr, $18.5 \mu\text{M}$ of Et gets released from the micelle by caffeine while $6.5 \mu\text{M}$ Et still remains attached to the micelle. As evidenced from the UV–vis absorption spectra along with the fluorescence lifetime and anisotropy measurements of Et at different concentrations of neutral (polar) surfactant TX-100 (details given in Supporting Information section, Figure S2 and Table S3), Et binds neither to TX-100 monomers nor to TX-100 micelles at lower concentrations ($8.2 \times 10^{-3} \text{ mM}$ micellar concentration). However, at high micellar concentration (1

mM), we observe a bathochromic shift in the absorption peak of Et compared to that in water, which reflects association of Et with the TX-100 micelle, with the quarternary nitrogen of Et toward the hydrophilic headgroup of the micelle, i.e., toward the ethylene oxide part (see Supporting Information section Figure S7), and with the hydrophobic part being buried inside. The proposed model corroborates with the fluorescence anisotropy results (Table S3 in Supporting Information section) where we find a longer rotational time constant of Et at 100 mM TX-100 concentration. However, detailed analysis of the absorption and time-resolved spectroscopy results show that caffeine fails to detach Et from the TX 100 micelle unlike SDS and CTAB micelles. Our DLS studies on differently charged micellar systems (Figure 1b) show the structural integrity of the micelles both in the absence and in the presence of caffeine. Because the hydrodynamic radii of the micelles remain similar even after the addition of caffeine, it can be concluded that caffeine molecules are not associated with the micelles. To show the detachment of Et at the molecular level from the anionic SDS micelles, which is considered to be mimic of the DNA surface,¹⁴ we have employed Förster resonance energy transfer (FRET) from another ligand H258 on the surface of the micelle to the bound Et. The FRET, which is known to be molecular ruler,²⁰ is an effective technique to find the distance between two ligands, donor and acceptor, having an overlap of the emission and absorption spectrum of the donor and acceptor, respectively. Figure 2 shows that there is sufficient spectral overlap between the emission spectrum of the H258 and the absorption spectrum of the Et in SDS micelles both in the absence and in the presence of caffeine. As shown in the figure, $J(\lambda)$, the overlap integral, which expresses

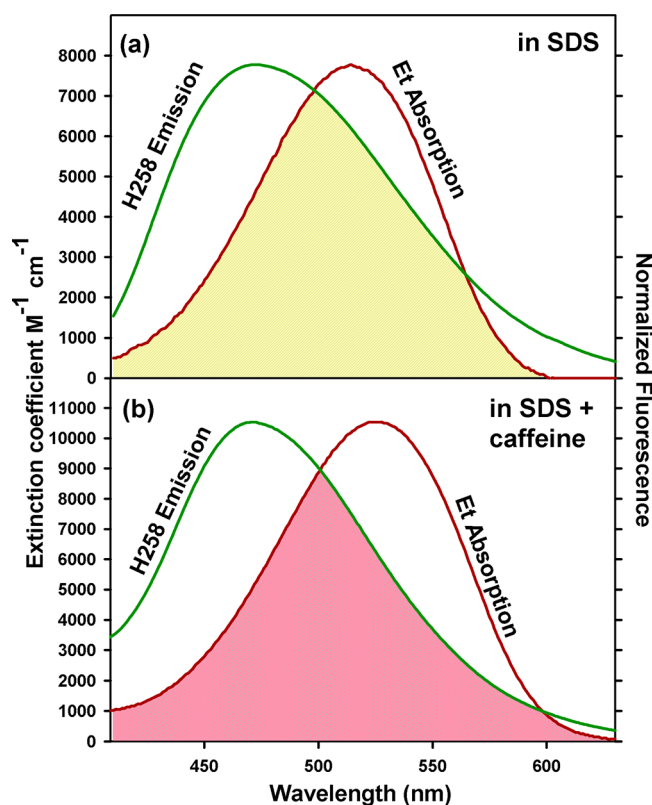


Figure 2. Spectral overlap of H258 emission and Et absorption in 20 mM SDS in the (a) absence and (b) presence of 100 mM caffeine.

the degree of spectral overlap between the donor emission and the acceptor absorption changes in the presence of caffeine.

The minor groove binder H258 shows single exponential fluorescence decay of 3.38 ns in the SDS micelle (Figure 3a,

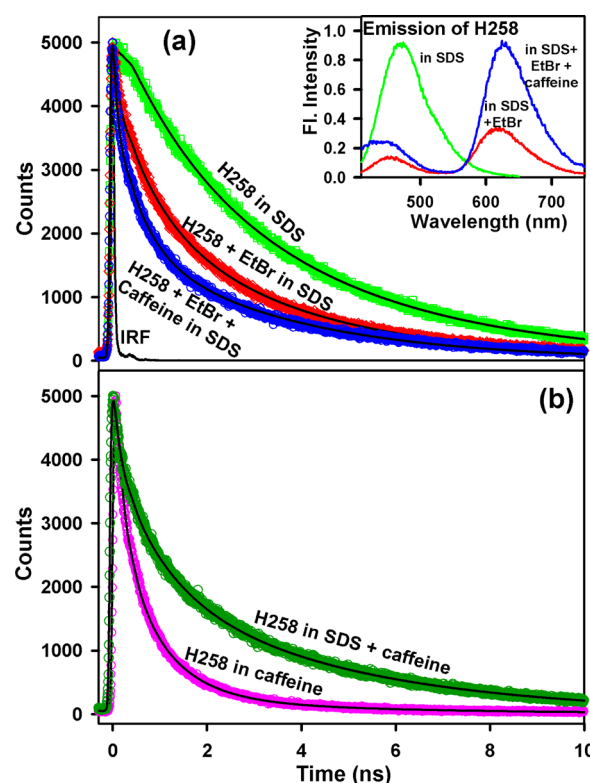


Figure 3. Temporal decays of H258 (0.2 μ M), H258–Et ([Et] = 155 μ M), and H258–Et–caffeine ([caffeine] = 100 mM) in (a) 20 mM SDS and that of H258–caffeine in (b) SDS and water. The emission spectra of H258, H258–Et, and H258–Et–caffeine in (inset a) SDS. All the samples are excited at λ_{ex} = 375 nm and fluorescence transients monitored at λ_{em} = 470 nm.

Table 2). Previous work from our group¹⁵ finds the location of H258 on the surface of the SDS micelle and not in the interior of it on the basis of steady-state emission and time-resolved anisotropy studies of the probe in the micellar environment. The presence of Et (acceptor) in the solution makes the decay faster (867 ps (17%) and 98 ps (2%)) (Table 2), revealing simultaneous binding of H258 and Et in the micellar surface

Table 2. Lifetime Components of H258 in Various Environments^a

sample	τ_1 (ns)	τ_2 (ns)	τ_3 (ns)
H258 in SDS	3.38 (100%)		
H258 in SDS + Et	3.38 (81%)	0.87 (17%)	0.1 (2%)
H258 in SDS + Et + caffeine	3.38 (80%)	0.55 (17%)	0.08 (3%)
H258 in SDS + caffeine	3.38 (91%)	0.36 (9%)	
H258 in water	3.82 (95%)	0.14 (5%)	
H258 in water + Et	3.82 (69%)	0.49 (21%)	0.09 (10%)
H258 in water + Et + caffeine	3.82 (34%)	0.14 (13%)	0.78 (53%)
H258 in water + caffeine	3.82 (31%)	0.81 (55%)	0.16 (14%)

^a τ represents the time constant, and the numbers in parentheses represent relative contribution of the component. [H258] = 0.2 μ M, [SDS] = 20 mM, [Et] = 155 μ M, and [caffeine] = 100 mM. Error \pm 5%.

with an average distance of 2.16 nm, consistent with earlier studies.¹⁷ The fast time component τ_3 listed in Table 2 is around IRF, however, within the resolution of our TCSPC setup (see Supporting Information, Figure S3). The binding of Et on the surface of the SDS micelle is also reasonable from the time-resolved studies reported earlier²¹ where the fluorescence lifetime and relative quantum yield of Et, bound to SDS, are shown to be intermediate between those in water and in alcohol reflecting that Et binds to the surface of the anionic SDS micelle due to its inherent positive charge. Upon addition of caffeine in solution the fluorescence decay becomes faster, apparently revealing closer association of H258 and Et (1.94 nm). Relative enhancement of the Et emission (steady state) in the H258 coated SDS micelle in the presence of caffeine (inset Figure 3a) is also in favor of the above conclusion. However, upon the addition of caffeine, FRET between H258 and Et is interrupted as Et is released from the micelle in the presence of caffeine and such interruption results in the increase in the fluorescence intensity of H258 band. As shown in Figure 3b and Table 2, fluorescence decay of H258 in the micelle becomes faster upon addition of caffeine as a consequence of partial detachment of H258 from the micellar surface. Thus, the fate of the H258–Et complex upon addition of caffeine is found to be inconclusive from the standard FRET analysis. We have repeated our experiment with another donor coumarin 500 (C500) which does not interact with caffeine at high temperature ($\sim 70^\circ\text{C}$), as has been reported by our earlier studies;²² however, both caffeine dimer and caffeine–Et complex have been reported by us to be stable even at high temperatures around 70°C .⁹ Hence, we repeated the experiments with the donor C500 at 70°C (details given in Supporting Information section, Figure S4 and S5, Table S4) and found that in the absence of caffeine 33% donor molecules participate in FRET with 87% energy transfer efficiency (E) whereas in the presence of caffeine only 19% donor molecules participate in FRET with E as 80%, which is due to the caffeine-mediated release of acceptor Et molecules from the SDS micelles. The donor–acceptor distance (r) also increases from 2.89 to 3.16 nm in the presence of caffeine.

For better understanding of the fate of the association between H258 and Et in the presence of caffeine, it is essential to know the distribution of Et molecules around the micelle before and after the addition of caffeine, because this is a governing factor for efficient energy transfer. The decay of excited probes in a micelle may be described by the following kinetic model, which is known as the Infelta–Tachiya model:^{23,24}



where P_n^* stands for a micelle containing an excited probe and n quencher molecules, whereas P_n stands for a micelle that contains n quencher molecules but no excited probe. k_0 is the total decay constant of the excited state in the absence of a quencher. k_q is the rate constant for quenching of an excited probe in a micelle containing one quencher molecule. Thus when a micelle containing a probe with n quencher molecules is excited, the rate constant for the excited-state decay of that probe is given by $k_0 + nk_q$ and the total energy transfer rate constant is nk_q . In this kinetic model, it is assumed that the

distribution of the number of quenchers attached to one micelle follows a Poisson distribution,²³ namely,

$$p(n) = (m^n/n!) \exp(-m) \quad (9)$$

where m is the mean number of quenchers in a micelle.

$$m = k_+[A]/k_- \quad (10)$$

where k_+ is the rate constant for entry of a quencher molecule into a micelle, whereas k_- is the rate constant for exit of a quencher molecule from a micelle containing one quencher molecule. A stands for a quencher molecule in the aqueous phase. Based upon the above model, the equation for the total concentration $P^*(t)$ of excited probes at time t is given by²⁵

$$P^*(t) = P^*(0) \exp \left[- \left(k_0 + \frac{k_0 k_+[A]}{k_- + k_q} \right) t - \frac{k_q^2 k_+[A]}{k_-(k_- + k_q)^2} \{ 1 - \exp[-(k_- + k_q)t] \} \right] \quad (11)$$

If k_- is much smaller than k_q , eq 11 reduces to

$$P^*(t) = P^*(0) \exp \{ -k_0 t - m[1 - \exp(-k_q t)] \} \quad (12)$$

In one of our systems, along with the Et quencher molecules, there exist some caffeine molecules that also cause quenching of the lifetime of the excited probe (H258) due to its partial release from the micelle and these are also taken into account. If the distribution of the number of caffeine-mediated detached donor molecules from the micellar surface follows Poisson distribution with the average number (m_c), the decay curves of the excited state of H258 in the micelle in the presence of caffeine without and with the Et molecules are described by²⁶

$$P^*(t) = P^*(0) \exp \{ -k_0 t - m_c[1 - \exp(-k_{qc} t)] \} \quad (13)$$

$$P^*(t) = P^*(0) \exp \{ -k_0 t - m_c[1 - \exp(-k_{qc} t)] - m[1 - \exp(-k_q t)] \} \quad (14)$$

where the quenching rate constant (k_{qc}) by caffeine molecules may be different from that (k_q) by Et molecules. We have determined the values of the parameters m_c , k_{qc} , k_0 , m , and k_q by fitting eqs 12–14 to the decay curves in the absence and presence Et and caffeine molecules (Figure 4 and Table 3). We have also employed extended Infelta–Tachiya kinetic model described by the following equation,²⁷

$$P^*(t) = P^*(0) \exp[-\gamma t + \mu(\exp^{-\beta t} - 1)] \quad (15)$$

where γ , μ , and β are functions of the rate constants of probe migration (k), quenching (k_q), and quencher exchange either by micelle collision (k_e) or via the aqueous phase (k_-) and are explicitly defined as

$$\gamma = k_0 + k + ma_2 k_q / \beta \quad (16)$$

$$\mu = m k_q^2 / \beta^2 \quad (17)$$

$$\beta = k_q + a_2 \quad (18)$$

$$a_2 = k_e[M] + k_- \quad (19)$$

In the expressions 16–19, k_0 , m , and $[M]$ stand for the deactivation rate constant of the excited probe in the absence of

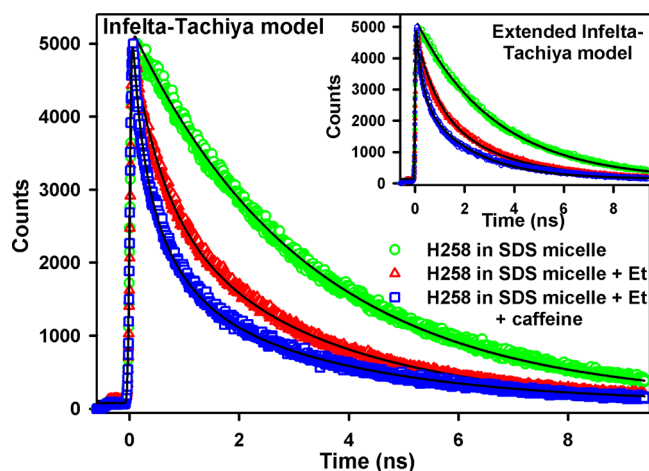


Figure 4. Time-resolved fluorescence decay curves of H258 in the SDS micelle in the absence and presence of caffeine and Et. The bold lines represent the fitting of the curves by the generalized version as well as the extended version (inset) of the kinetic models developed by Infelta and Tachiya (see text).

Table 3. Values of the Quenching Parameters Using the Simplified Version of the Model Developed by Infelta–Tachiya

system	k_0 (ns^{-1})	m	k_q (ns^{-1})	m_c	k_{qc} (ns^{-1})
micelle bound H258	0.31				
micelle bound H258 + Et	0.31	0.66	1.08		
micelle bound H258 + Et + caffeine	0.31	0.31	5.34	0.89	1.11

quencher, the average number of quenchers per micelle, and the micelle concentration, respectively. The quenching parameters k_0 , m , and k_q derived from the extended Infelta–Tachiya model (Figure 4 inset and Table 4) were found to be comparable with those derived from the generalized version of Infelta–Tachiya model.

Table 4. Values of the Quenching Parameters Using the Extended Version of the Model Developed by Infelta–Tachiya

system	k_0 (ns^{-1})	k_q (ns^{-1})	m	k_{qc} (ns^{-1})
micelle bound H258	0.31			
micelle bound H258 + Et	0.31		0.82	0.57
micelle bound H258 + Et + caffeine	0.31	0.17	0.69	2.92

Figure 4 shows the time-resolved fluorescence transients of H258 in the absence and presence of caffeine and Et molecules, fitted with eqs 12–14 whereas Figure 4 inset shows the same fitted with eq 15. The observed fluorescence transients were fitted using a nonlinear least-squares fitting procedure (software SCIENTIST) to a function $X(t) = \int_0^t E(t') P(t-t') dt'$ comprising the convolution of the instrument response function (IRF) ($E(t)$) with exponential ($P(t) = P(0) \exp\{-k_0 t - m_c[1 - \exp(-k_q t)] - m[1 - \exp(-k_{qc} t)]\}$). The purpose of this fitting is to obtain the decays in an analytic form suitable for further data analysis. As evident from the figure, the models describe the decay curves reasonably well. The quenching parameters are summarized in Tables 3 and 4. Upon fitting the decay curves of H258 with the kinetic models mentioned

before, it is clear that the distribution of Et molecules on the micellar surface changes significantly after the addition of caffeine. As summarized in Tables 3 and 4, the mean number of Et molecules associated with the micelle (m) reduces after the addition of caffeine. Thus caffeine shows efficiency in the detachment of Et from the micellar surface. The quenching rate constant (k_q) due to the acceptor (Et) molecules increases in the presence of caffeine, revealing closer association between the remaining Et and H258 molecules on the micellar surface, which is consistent with the results obtained from FRET study and steady-state emission spectroscopy as mentioned before. However, standard FRET analysis failed to monitor the detachment of the bound Et molecules from the micellar surface in the presence of caffeine quantitatively. We have also employed Infelta–Tachiya model on our FRET study using C500 as the donor, which does not interact with caffeine molecules at the experimental conditions²² (details given in the Supporting Information section, Figure S6 and Table S5). The results clearly show a decrease in the mean number of Et molecules associated with the micelle upon addition of caffeine due to the caffeine-mediated release of Et from the SDS micelle. Furthermore, we determine the equilibrium constant for solubilization of Et in SDS micelles before and after the addition of caffeine. The total concentrations $[M]$ and $[Q]$ of the micelle and Et introduced in solution are related through the following equation,

$$m[M] + [A] = [Q] \quad (20)$$

$$m = k_+[A]/k_- \quad (21)$$

where $[A]$ is the concentration of Et in the aqueous phase. Elimination of $[A]$ from eqs 20 and 21 yields

$$K = k_+/k_- = m/([Q] - m[M]) \quad (22)$$

where K is the equilibrium constant (k_+/k_-) for the solubilization of Et in micelles and calculated to be 2.3×10^4 and $3.3 \times 10^3 \text{ M}^{-1}$ in the absence and presence of caffeine, respectively. K values have been calculated for different concentrations of Et in the absence of caffeine and have been found to be similar. The significant decrease in the value of equilibrium constant (K) for solubilization of Et in the micelle upon addition of caffeine confirms the efficacy of caffeine molecules in the detachment of Et from biomimetic systems like micelles.

Significant perturbation of FRET efficiency from the donor H258 to the acceptor Et has been revealed even from our cellular studies. Figure 5 shows the fluorescence micrographs of the squamous epithelial cells stained with both the donor (H258) and the acceptor (Et) fluorophores. The donor emits in the blue region of the visible spectrum (Figure 2) whereas the acceptor emits in the red region of the same. H258 and Et, being well-known DNA minor groove binder²⁸ and DNA intercalator,^{16,17} respectively, and both being cell permeable,^{9,29} stain the nuclei of the cells. Upon specifically exciting the donor dye molecules under UV light at 360 nm, we observe only the red (acceptor) emission from the nuclei of the cells, which emphasizes the FRET from the donor to the acceptor. However, as shown in Figure 5, upon the addition of caffeine (+ caffeine), we find the red emission from the acceptor changes to the blue emission of the donor with time, showing significant perturbation in the FRET efficiency between the two. Photobleaching of the donor (H258) and acceptor (Et) molecules both in the absence and in the presence of caffeine

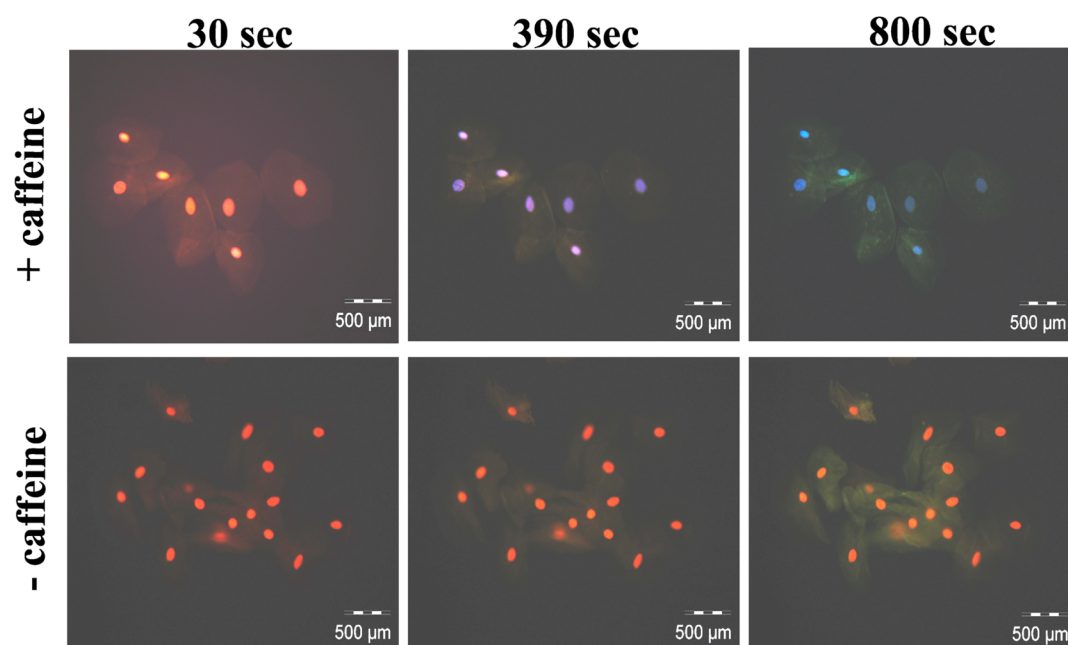


Figure 5. Fluorescence micrographs of squamous epithelial cells doubly stained with H2S8 and Et after 30, 390, and 800 s upon treatment with caffeine (+ caffeine) along with the control sets (– caffeine) treated with PBS without caffeine.

have been monitored by us in our control studies (data not shown) where we find no signature of acceptor photobleaching both in the absence and in the presence of caffeine within the experimental time frame. Donor H2S8 molecules also do not undergo photobleaching in the presence of caffeine but significant photobleaching of the donor molecules in the absence of caffeine has been observed. It has to be noted that the emission intensity of the donor even after 800 s of caffeine treatment is less than that in the absence of the acceptor (image not shown) most probably due to the fraction of acceptor molecules that still remained in the micelle even after the addition of caffeine. The possibility of removal of some of the donor molecules from the nucleus cannot be ruled out, whereas, in the control experiment, in which the cells were treated only with the phosphate buffer saline (PBS) without caffeine (– caffeine), we find no significant change in the red emission from the nuclei with time. To highlight the observed perturbation in FRET efficiency from H2S8 to Et in the presence of caffeine in a more quantitative manner, the average intensity of the red (acceptor) and blue (donor) emission from the nuclei in each micrograph has been plotted against time for both test (+ caffeine) and control (– caffeine) experiments, as shown in Figure 6a,b, respectively. In Figure 6a, the drop in emission intensity of the acceptor with time has been fitted biexponentially (within $\pm 10\%$ error) with the characteristic time constants of 122 and 550 s, which exactly coincides with that of the biexponential fit of the rise of the donor emission intensity with time within the error limit. As shown in Figure 6b, in control experiment (– caffeine) there is a slight decrease in the red emission intensity of the acceptor due to the partial detachment of Et from the cell nuclei by the PBS buffer, which leads to the slight increase in the blue emission intensity of the donor. As we observe a slight increase in the blue fluorescence intensity of the donor it can be concluded that the donor H2S8 molecules undergo photobleaching at a much slower rate compared to the buffer-mediated release of nonspecifically bound EtBr. The respective decay and rise of the acceptor and

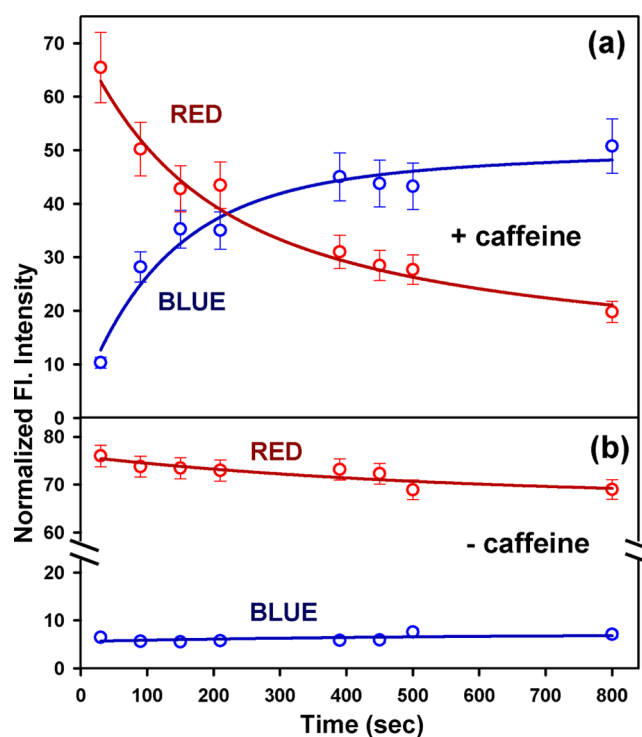


Figure 6. Rate of change in the intensity of red and blue emission from the doubly stained squamous epithelial cells (a) upon treatment with caffeine (+ caffeine) and (b) upon treatment with PBS without caffeine (– caffeine) taken as control.

donor can be fitted single exponentially within the same error limit with a characteristic time component of 550 s, which coincides with the slower time component obtained in the presence of caffeine. Thus this slower time component of 550 s can be assigned to the caffeine independent release of Et from the cell nuclei by the buffer itself and the faster time component (122 s) is achieved solely due to the presence of caffeine.

Therefore, the caffeine-mediated release of the bound Et from cell nuclei is almost 5 times faster compared to that with the solvent alone. It has to be noted that the time constant for the release of Et from the nuclei of squamous epithelial cells reported here, is much slower than that proposed in our earlier work,⁹ which accounts for the lower caffeine concentration purposely used in our present work to vividly show the alteration of FRET.

CONCLUSION

Our study finds caffeine as an efficient drug for the removal of a model DNA–intercalator Et from both negatively charged SDS and positively charged CTAB micelles without or with negligible perturbation of their structural integrity. However, caffeine fails to show such activity in the case of neutral (polar) TX-100 micelles. The FRET study focuses on the efficacy of caffeine molecules in altering the association between two DNA binding ligands H258 and Et residing on a micellar surface. However, in our system, standard FRET fails to provide an explicit picture of such alteration in the association between the two DNA-binding ligands on the biomimetic system in the presence of caffeine. Our analysis of the experimental results employing the well established kinetic model developed by Infelta and Tachiya, helps to recognize the efficacy of caffeine molecules in the detachment of Et from the biomimetic system. The result of our cellular studies further emphasizes on the perturbation of FRET efficiency from H258 to Et in the presence of caffeine. Our study may help to carry out further experiments in the fields of medicine where caffeine can be taken as an active ingredient to protect cells from various cell damaging agents like DNA-intercalators.

ASSOCIATED CONTENT

Supporting Information

The details of time-resolved fluorescence results along with those of fluorescence anisotropy of ethidium (Et) in a wide range of CTAB concentrations (0.2–80 mM) both in the absence and in the presence of caffeine; absorbance, steady-state, and time-resolved emission along with the fluorescence anisotropy of Et at different concentrations of SDS and TX-100 both in the absence and in the presence of caffeine; resolution of time-correlated single photon counting (TCSPC) setup; Förster resonance energy transfer (FRET) between coumarin 500 (C500) and Et on SDS micelles in the absence and presence of caffeine; and structures of the alkaloid, dyes, and surfactants used in the study. This material is available free of charge via the Internet at <http://pubs.acs.org>.

AUTHOR INFORMATION

Corresponding Author

*E-mail: skpal@bose.res.in. Fax: 91 33 2335 3477.

Notes

The authors declare no competing financial interest.

ACKNOWLEDGMENTS

S.B. thanks UGC for Research Fellowship. We thank DST for a financial grant (SR/SO/BB-15/2007).

REFERENCES

- (1) Selby, C. P.; Sancar, A. *Proc. Natl. Acad. Sci.* **1990**, *87*, 3522–3525.
- (2) Traganos, F.; Kapuscinski, J.; Darzynkiewicz, Z. *Cancer Res.* **1991**, *51*, 3682–3689.
- (3) Kapuscinski, J.; Kimmel, M. *Biophys. Chem.* **1993**, *46*, 153–163.
- (4) Davies, D. B.; Veselkov, D. A.; Djimant, L. N.; Veselkov, A. N. *Eur. Biophys. J.* **2001**, *30*, 354–366.
- (5) Larsen, R. W.; Jasuja, R.; Hetzler, R. K.; Muraoka, P. T.; Andrada, V. G.; Jameson, D. M. *Biophys. J.* **1996**, *70*, 443–452.
- (6) Piosik, J.; Zdunek, M.; Kapuscinski, J. *Biochem. Pharmacol.* **2002**, *63*, 635–646.
- (7) Bedner, E.; Du, L.; Traganos, F.; Darzynkiewicz, Z. *Cytometry* **2001**, *43*, 38–45.
- (8) Johnson, I. M.; Kumar, S. G. B.; Malathi, R. J. *Biomol. Struct. Dyn.* **2003**, *20*, 677–685.
- (9) Banerjee, S.; Bhowmik, D.; Verma, P. K.; Mitra, R. K.; Sidhanta, A.; Basu, G.; Pal, S. K. *J. Phys. Chem. B* **2011**, *115*, 14776–14783.
- (10) Traganos, F.; Kaminska-Eddy, B.; Darzynkiewicz, Z. *Cell Prolif.* **1991**, *24*, 305–319.
- (11) Turro, N. J.; Grätzel, M.; Braun, A. M. *Angew. Chem. Intern. Ed.* **1980**, *19*, 675–696.
- (12) Zhong, D.; Pal, S. K.; Zewail, A. H. *Chem. Phys. Chem.* **2001**, *2*, 219–227.
- (13) Pal, S. K.; Peon, J.; Zewail, A. H. *Proc. Natl. Acad. Sci. U. S. A.* **2002**, *99*, 1763–1768.
- (14) Mitra, R. K.; Sinha, S. S.; Pal, S. K. *J. Fluoresc.* **2008**, *18*, 423–432.
- (15) Banerjee, D.; Pal, S. K. *Chem. Phys. Lett.* **2006**, *432*, 257–262.
- (16) Sarkar, R.; Pal, S. K. *Biopolymers* **2006**, *83*, 675–686.
- (17) Banerjee, D.; Pal, S. K. *J. Phys. Chem. B* **2007**, *111*, 5047–5052.
- (18) Mahler, H. R.; Perlman, P. S. *Arch. Biochem. Biophys.* **1972**, *148*, 115–129.
- (19) Lakowicz, J. R. *Principles of fluorescence spectroscopy*; Kluwer Academic/Plenum: New York, 1999.
- (20) Shaw, A. K.; Sarkar, R.; Pal, S. K. *Chem. Phys. Lett.* **2005**, *408*, 366–370.
- (21) Pal, S. K.; Mandal, D.; Bhattacharyya, K. *J. Phys. Chem. B* **1998**, *102*, 11017–11023.
- (22) Banerjee, S.; Verma, P. K.; Mitra, R. K.; Basu, G.; Pal, S. K. *J. Fluoresc.* **2012**, *22*, 753–769.
- (23) Tachiya, M. *Chem. Phys. Lett.* **1975**, *33*, 289–292.
- (24) Infelta, P. P.; Grätzel, M.; Thomas, J. K. *J. Phys. Chem.* **1974**, *78*, 190–195.
- (25) Tachiya, M. *J. Chem. Phys.* **1982**, *76*, 340–348.
- (26) Sadhu, S.; Halder, K. K.; Patra, A. J. *J. Phys. Chem. C* **2010**, *114*, 3891–3897.
- (27) Gehlen, M. H.; Auweraer, M. V.; Schryver, F. C. D. *Langmuir* **1992**, *8*, 64–67.
- (28) Sarkar, R.; Pal, S. K. *Biomacromolecules* **2007**, *8*, 3332–3339.
- (29) Chen, T. R. *Exp. Cell Res.* **1977**, *104*, 255–262.